J Polym Res (2012) 19:9889
DOI 10.1007/s10965-012-9889-2

ORIGINAL PAPER

Thermo-mechanical properties of high density polyethylene – fumed silica nanocomposites: effect of filler surface area and treatment

A. Dorigato · M. D'Amato · A. Pegoretti

Received: 17 February 2011 / Accepted: 23 August 2011
© Springer Science+Business Media B.V. 2012

Abstract High density polyethylene was melt compounded with various untreated (hydrophilic) or surface treated (hydrophobic) fumed silica nanoparticles, having different surface areas. The thermo-mechanical properties of the resulting nanocomposites have been thoroughly investigated. Field emission scanning electron microscopy revealed that nanofiller aggregation was more pronounced as the silica surface area increased, while nanofiller dispersion improved with a proper filler functionalization. The homogeneous distribution of fumed silica aggregates at low filler content allowed us to reach remarkable improvements of thermal stability, evidenced by an increase of the degradation temperature and a decrease of the mass loss rate with respect to neat matrix, especially when surface treated nanoparticles were utilized. Interestingly, the stabilizing effect produced by fumed silica nanoparticles was accompanied by noticeable enhancements of the ultimate tensile mechanical properties, both under quasi-static and impact conditions. Concurrently, a progressive enhancement of both elastic modulus and tensile stress at yield with the filler amount, was observed.

Keywords Polyethylene · Silica · Polymer nanocomposites · Mechanical properties · Creep

A. Dorigato (✉) · M. D'Amato · A. Pegoretti
Department of Materials Engineering and Industrial Technologies and INSTM Research Unit, University of Trento,
via Mesiano 77,
38123 Trento, Italy
e-mail: andrea.dorigato@ing.unitn.it

Introduction

A rising interest has recently emerged for the use of nanostructured materials such as silica, titania, carbon nanotubes and layered silicates as fillers able to profoundly modify the properties of polymeric matrices [1, 2]. In fact it has been widely proven that the addition of small amounts of nanofillers (usually less than 10 wt%) to polymers can improve their mechanical properties (such as stiffness [3, 4], ultimate properties [5, 6], dimensional stability under creep conditions [7, 8]), their gas and solvents barrier properties [9] and their thermal degradation and chemical resistance [10]. Moreover, the drawbacks typically associated to the addition of traditional microfillers, such as embrittlement and loss of optical clarity, can be generally avoided [11].

Because of its combination of low cost, high chemical resistance, and well balanced mechanical properties, high density polyethylene (HDPE) is one of the most widely used thermoplastics. For some applications, such as pipes and fittings for liquids or gases transportation, the long-term creep mechanical response is one of the most important properties to be considered. The relatively poor stiffness and creep resistance of polyethylene, accompanied by its limited thermal stability, may represent a severe limitation. Introduction of relatively small amounts of nanoparticles has been proven to effectively improve the creep stability of polymer matrices [12, 13].

Bondioli et al. investigated the effects of submicrometric titania particles on the tensile mechanical properties of a HDPE matrix, evidencing an interesting reduction of its creep compliance [1, 2]. Sudar et al. investigated the

Published online: 31 May 2012

mechanism and kinetics of void formation and growth in calcium carbonate ($CaCO_3$) filled polyethylene nanocomposites, finding a general enhancement of the quasi-static tensile properties with the filler content [14]. Zhang et al. studied the mechanical role of grafted silica nanoparticles in high density polyethylene composites prepared by melt compounding, showing a rise in tensile stiffness, tensile strength and impact strength of the composites and evidencing how the introduction of the grafting polymers onto the nanoparticles could increase the tailorability of the composites [5].

Quite surprisingly, only a few papers can be found on polyethylene - fumed silica nanocomposites. Fumed silica nanoparticles exist in a wide range of size (specific area ranging from 50 to 400 $m^2\ g^{-1}$) and with a variety of surface treatments from hydrophilic to hydrophobic. Due to their fractal structure and their high specific area, fumed silica is subjected to self-aggregation and it can consequently form a network of connected or interacting particles in polymers [15]. As recently reported by this research group, the mechanical performances of various thermoplastic matrices, such as linear low-density polyethylene (LLDPE) [16], polymethylpentene [17], and cycloolefin copolymers [18] can be substantially improved by the introduction of fumed silica nanoparticles, without sacrifying their optical transparency. Also Kontou demonstrated the potential of fumed silica nanoparticles in improving the stiffness and toughness of LLDPE prepared using both metallocene and Ziegler–Natta catalysts, with a strong dependence on the surface area of the nanofillers [19]. In a similar work, we have recently shown how the introduction of nanosilica having different surface area values could markedly affect the rheological [15] and creep behaviour [16] of an LLDPE matrix, and an extended modelization activity on the viscoelastic properties of the resulting materials both in the molten and solid states was proposed.

In this work, HDPE-fumed silica nanocomposites have been investigated with a focus on the role played by the filler surface area, surface functionalization and filler content on the thermo-mechanical behaviour. Particular attention was devoted to the thermal degradation stability and to the tensile behaviour of the resulting composites both under quasi-static and creep conditions.

Experimental

Materials

Fine powders of an Eltex A4009 MFN1325 (Ineos Polyolefins, UK) HDPE with a density of 0.96 $g{\cdot}cm^{-3}$, a melting temperature of 136 °C, a melt flow rate of 0.9 $g{\cdot}(10\ min)^{-1}$ (at 190 °C, 2.16 kg), were used. Various kinds of Aerosil® fumed silica nanoparticles, supplied by Degussa (Hanau, Germany), were utilized as nanofillers. Selected nanoparticles were different in terms of surface area values: 90 $m^2\ g^{-1}$ for Aerosil® 90, 200 $m^2\ g^{-1}$ for Aerosil® 200, and 380 $m^2\ g^{-1}$ for Aerosil 380. Moreover, silica nanoparticles surface treated with dimethyldyclorosilane (Aerosil® r974), having a surface area of 170 $m^2\ g^{-1}$, were also used. For all nanoparticles the SiO_2 content was higher than 99.8 %. Table 1 summarizes the most important properties of these nanofillers. Both matrix and nanoparticles were utilized as received.

Sample preparation

Polyethylene–silica nanocomposites were prepared by a melt compounding process, using a Haake PolyLab system consisting of a Rheomix 600 internal mixer and a Rheocord 300p control module for continuous monitoring of torque, motor speed and temperature. Both polyethylene and the selected amount of nanopowder (total mass of about 50 g) were inserted in the compounder and melt-mixed for 10 min at a temperature of 155 °C and rotor speed of 60 rpm. The compounded materials were then extracted and left to cool down to ambient temperature. Square sheets (side 200 mm and thickness 0.8 mm) were then obtained by compression molding for 10 min at 155 °C in a Carver laboratory press under an applied pressure of 0.2 kPa. The materials were then water cooled at 20 °C min^{-1}. In this way, neat matrix and nanocomposite samples filled with various types of silica at a constant filler loading of 2 vol% were prepared. Aerosil® r974 filled composites displayed the best balance between thermal and mechanical properties, therefore this nanofiller was selected for the preparation of nanocomposites with different silica amounts in the range from 1 vol% to 8 vol%. Nanocomposites were

Table 1 Physical properties of Aerosil® fumed silicas utilized in this work

	Aerosil® 90	Aerosil® 200	Aerosil® 380	Aerosil® r974
Specific surface area ($m^2\ g^{-1}$)	90±15	200±25	380±30	170±20
Primary nanoparticles diameter (nm)	20	12	7	12
Density[a] ($g{\cdot}cm^{-3}$)	2.50	2.28	2.41	1.99
Surface treatment	none	none	none	dimethyldyclorosilane

[a] Measured through an Accupyc® 1330 helium pycnometer

designated as HDPE followed by the silica type and the filler content. As an example, HDPE-A200-2 indicates a nanocomposite sample filled with 2 vol% of Aerosil® 200 fumed silica.

Experimental methodologies

Field emission scanning electron microscope (FESEM) observations were taken through a Zeiss Supra 40 microscope, operating at an acceleration voltage of 10 kV. Samples were cryofractured in liquid nitrogen and observed at different magnifications after metallization.

Differential scanning calorimetry (DSC) tests were performed by using a Mettler® DSC30 apparatus, testing small specimens cut from the square sheets and having a mass of 30 mg. Samples were first heated from 0 °C to 200 °C, then cooled to 0 °C and finally reheated up to 200 °C. All scansions were performed at 10 °C min^{-1} under a nitrogen flow of 100 ml min^{-1}. The crystallinity amount was computed normalizing the melting enthalpy values over the standard enthalpy of the fully crystalline polyethylene, taken as 293 Jg^{-1} [20]. Thermogravimetric analysis (TGA) were conducted in a Mettler TG50 thermobalance in a temperature range from 30 °C to 700 °C at a heating rate of 10 °C min^{-1} under an oxygen flow of 100 ml·min^{-1}.

Quasi-static tensile tests were performed at room temperature by using an Instron® 4502 tensile testing machine on ISO 527 1BA dogbone samples, 5 mm wide and 0.8 mm thick. Elastic modulus was evaluated at a crosshead speed of 0.25 mm min^{-1}, and the strain was recorded through an Instron 2620–601 extensometer at a gage length of 12.5 mm. According to ISO 527 standard, the elastic modulus was determined as a secant value between deformation levels of 0.05 % and 0.25 %. Ultimate tensile properties were determined at a crosshead speed of 50 mm min^{-1} without using the extensometer, and the deformation was monitored normalizing the crosshead displacement over the gage length of the samples (30 mm). At least five specimens were tested for each sample. Short term (3600 s) tensile creep tests were performed at 30 °C by using a TA Instruments DMA Q800 dynamic analyzer on rectangular samples 20 mm long, 6 mm wide and 0.8 mm thick. A tensile creep compliance D(t) was computed dividing the time dependent strain $\varepsilon(t)$ by the constant stress (σ_0) fixed as 10 % of the tensile stress at yield of neat PE.

Results and discussion

Microstructural characterization

A detailed investigation of the nanofiller morphology within the matrix is a key parameter to impart desired mechanical properties of polymer nanocomposites. FESEM micrographs of 2 vol% nanocomposites reported in Fig. 1 put in evidence that fumed silica nanoparticles tend to form agglomerates in the PE matrix, with a mean diameter of less than 300 nm. This feature is very common when untreated fumed silica nanoparticles are dispersed in polyolefin matrices, and can be

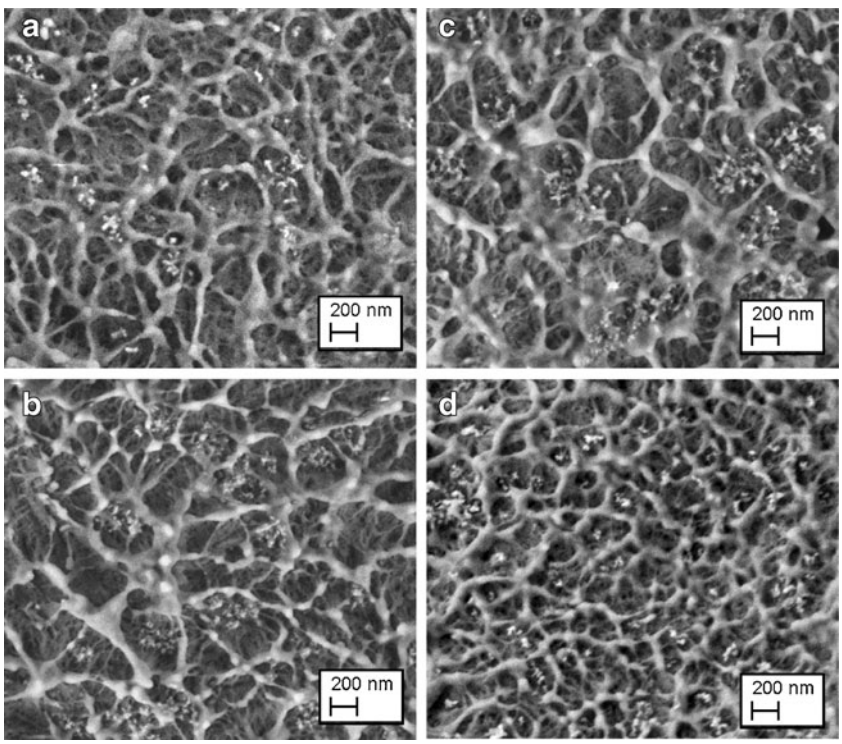

Fig. 1 FESEM micrographs of **a** PE-A90-2, **b** PE-A200-2, **c** PE-A380-2, **d** PE-Ar974-2 nanocomposites

attributed to the strong interaction of the surface hydroxyl groups of fumed silica nanoparticles. Consequently, fumed silica form aggregates than can be hardly broken down during melt-mixing, even at high shear rates [21, 22]. Comparing aggregates morphology in hydrophilic fumed silica nanocomposites (Fig. 1a–c), it can be concluded that their size increases with the nanofiller surface area. In fact, HDPE-A90-2 sample is characterized by the presence of aggregates with a mean diameter of about 130 nm, whereas in HDPE-A200-2 and HDPE-A380-2 nanocomposites aggregates having respectively a mean size of about 210 nm and 240 nm can be observed. As mentioned before, this evidence can be explained considering that the agglomeration tendency of primary nanoparticles, due to the presence of hydroxyls groups on the surface of the nanofiller, increases with their surface area [22]. On the other hand, functionalized nanoparticles appear to be better dispersed in the PE matrix, forming aggregates with a mean diameter of about 80 nm. It can be therefore inferred that the presence of organosilane on the surface of the nanoparticles, improving the miscibility between organic and inorganic phases, prevents their agglomeration during the compounding process [23].

In Fig. 2 FESEM images of Aerosil r974 filled nanocomposites with different filler amounts are reported. It can be observed that fumed silica nanoparticles are uniformly dispersed in the matrix at all the investigated filler concentrations, forming isodimensional clusters of aggregated primary nanoparticles having a mean size lower than 200 nm. Even in this case, it is difficult to assess whether the clusters are constituted by aggregation of primary nanoparticles fused together during the manufacturing process or if they are formed by physical agglomeration of aggregates. However, the mean size of the aggregates is proportional to the filler content. HDPE-Ar974-1 sample is characterized by the presence of aggregates having a mean diameter of about 70 nm, while the mean dimension of silica aggregates in HDPE-Ar974-2 nanocomposite is slightly higher (about 80 nm). Nanocomposites at filler loadings of 4 vol% and 8 vol% show aggregates having a mean diameter of respectively 110 and 150 nm. As mentioned before, the aggregated morphology, characteristic of fumed silica nanoparticles, can be attributed to the strong interaction between the surface hydroxyl groups of the nanoparticles. Increasing the filler amount the mean distance between silica aggregates diminishes and the probability of nanofiller aggregation is therefore enhanced.

Thermal properties

In Fig. 3 DSC thermograms of 2 vol% nanofilled samples are compared with that of the pure matrix, while in Table 2 melting temperatures and relative crystallinity values during the heating and the cooling stages are reported. It is possible to observe that crystallization temperatures are slightly affected by the

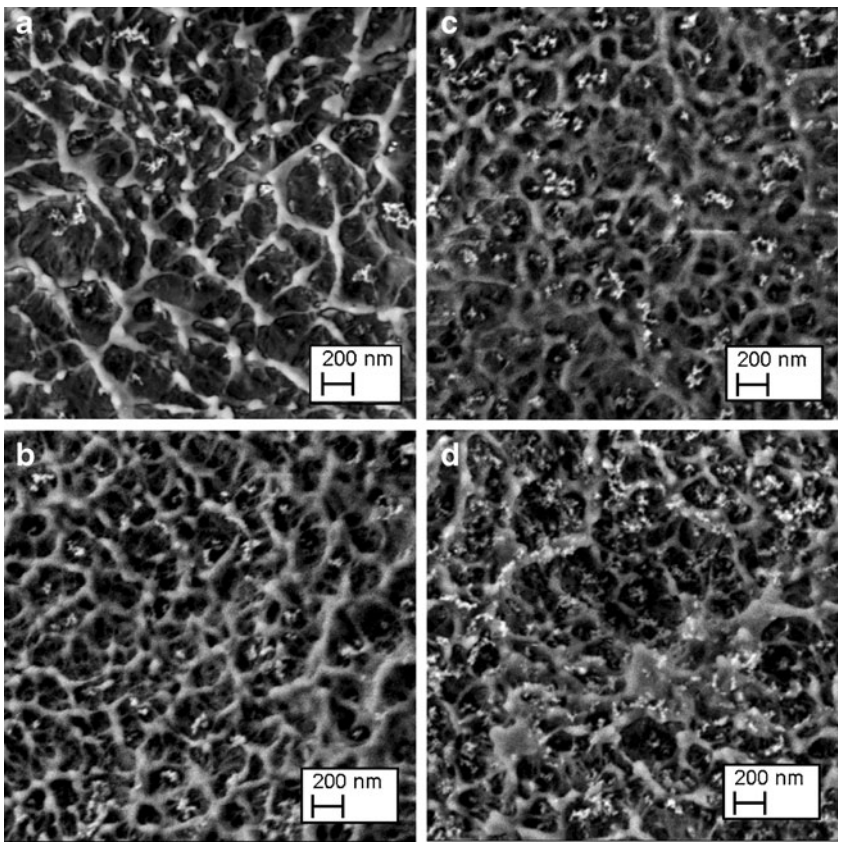

Fig. 2 FESEM micrographs of **a** PE-Ar974-1, **b** PE-Ar974-2, **c** PE-Ar974-4, **d** PE-Ar974-8 nanocomposites

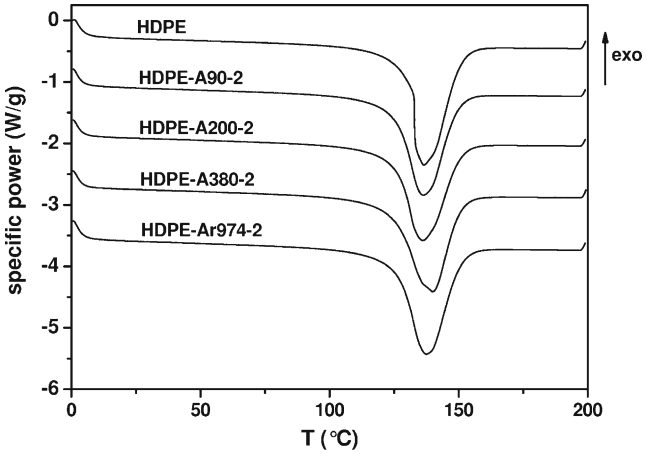

Fig. 3 DSC thermograms of neat HDPE and nanocomposites with 2 vol% filler content

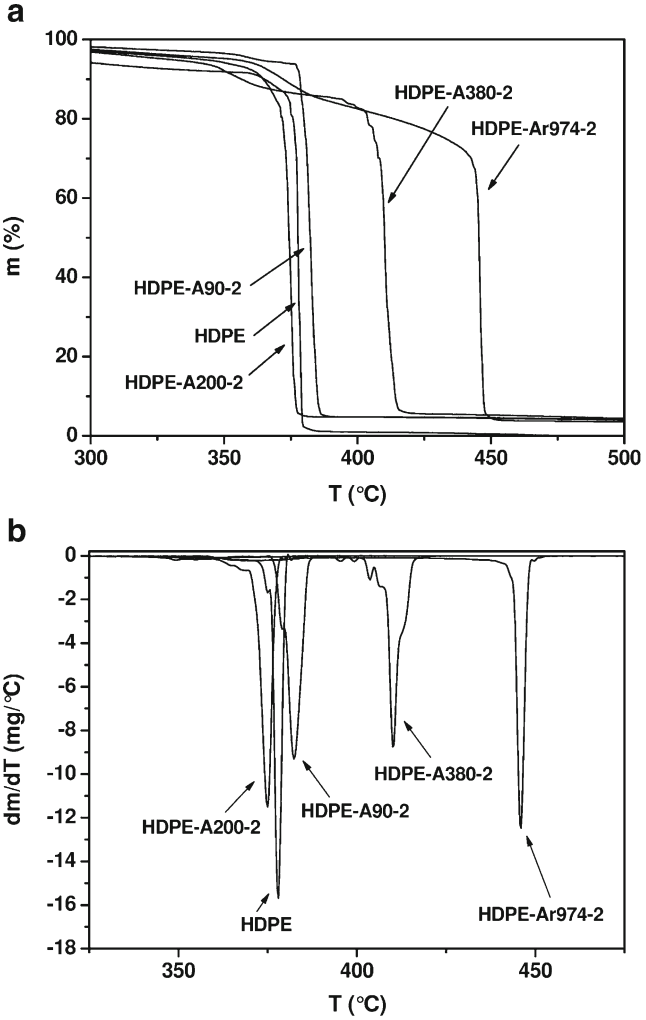

Fig. 4 TGA thermograms of neat HDPE and nanocomposites with 2 vol% filler content: **a** mass loss, **b** derivative of the mass loss

presence of fumed silica nanoparticles, without a clear dependency from the nanofiller surface area or from the presence of the organomodifier. For instance, T_c of HDPE-A380-2 nanocomposite is about 1 °C higher than that of the neat matrix. This probably means that, despite their amorphous nature, fumed silica nanoparticles having higher surface area could play some nucleating effect on the HDPE matrix. However, further investigations are needed to reach a better comprehension of the crystallization phenomena in these nanocomposite systems.

In Fig. 4a thermogravimetric curves of neat PE and related nanocomposites are reported, while in Fig. 4b the derivative of the mass loss values are represented. It can be seen that all the samples show a single degradation step at temperatures higher than 370 °C, in which the maximum mass loss rate is reached. While the remaining mass at 700 °C of the nanofilled samples is very close to the theoretical nanosilica weight percentage (about 5 wt%), the residue left after combustion of neat PE is nearly zero, as all the organic components decompose into gaseous products. The beneficial effects of fumed silica nanoparticles on the thermal degradation resistance of the nanocomposites is clearly evident considering the data reported in Table 3. Both $T_{2\%}$ and $T_{5\%}$ are positively affected by nanofiller introduction, while T_d is sensibly improved only by using A380 and Ar974 nanoparticles. Considering experimental uncertainties associated to these measurements, it is possible to assess that T_d values of A90 and A200 filled nanocomposites are practically equal to that of the neat resin. It is worthwhile to note that the introduction of 2 vol% of Aerosil® r974 causes an increase of T_d of about 70 °C. Also the maximum mass loss rate (MMLR) is noticeably lowered by the nanofiller addition. Analyzing these data from a general point

Table 2 DSC results on polyethylene-fumed silica nanocomposites (filler content =2 vol%)

Sample	T_{m1} (°C)	X_1 (%)	T_c (°C)	X_c (°C)	T_{m2} (°C)	X_2 (°C)
HDPE	136.4	65.3	116.3	67.9	136.7	69.6
HDPE-A90-2	136.3	65.2	115.2	67.6	136.8	69.3
HDPE-A200-2	136.0	64.6	116.3	66.5	135.6	67.6
HDPE-A380-2	139.9	65.5	117.2	66.6	135.8	67.8
HDPE-AR974-2	137.5	68.9	115.5	69.8	137.5	71.5

T_{m1} melting temperature - first heating, X_1 cristallinity content - first heating, T_c crystallization temperature - cooling, X_c cristallinity content – cooling, T_{m2} melting temperature - second heating, X_2 cristallinity content - second heating

Table 3 Results of TGA measurements on polyethylene-fumed silica nanocomposites under oxygen atmosphere (filler content =2 vol%)

Sample	$T_{2\%}$ (°C)	$T_{5\%}$ (°C)	T_d (°C)	MMLR (mg·°C^{-1})
HDPE	258	289	378	15.8
HDPE-A90-2	306	362	382	9.2
HDPE-A200-2	284	342	375	11.4
HDPE-A380-2	281	330	410	8.9
HDPE-Ar974-2	290	354	446	12.7

MMLR maximum mass loss rate, $T_{2\%}$ T associated to a weight loss of 2%, $T_{5\%}$ T associated to a weight loss of 5%, T_d decomposition temperature

of view, a remarkable stabilizing effect of silica nanoparticles on the thermal stability of HDPE under oxidizing conditions can be thus detected. According to the general theories on the flame resistance of polymeric nanocomposites [24, 25], it can be hypothesized that silica nanoparticles may act as thermal insulator and limit the diffusion of oxygen in the polymer matrix, making the diffusion path of the oxygen more tortuous thus retarding the thermo-oxidative process. During the thermal degradation of the polymer the silica aggregates tend to agglomerate to the surface of the molten polymer, thus creating a barrier that physically protects from heat the remaining polymer and hinders the volatilization of the oligomers generated during the combustion. According to FESEM images reported in Fig. 1, the relatively fine dispersion of functionalized silica aggregates, reducing the mean distance between the aggregates, permits the formation of a more efficient shield against oxygen diffusion [23]. The positive effect induced by Aerosil® r974 is partially counterbalanced by the relatively high organic load of organomodified silicas, since organic groups at low molecular weight are thermally less stable than polymer chains [26]. This could explain why $T_{2\%}$ and $T_{5\%}$ values of HDPE-Ar974-2 sample are very similar to that of hydrophilic fumed silica composites. On the other hand T_d temperature, associated to the maximum mass loss rate, strongly depends on the nanofiller dispersion within the matrix. The lower aggregation degree of organomodified silicas shown in ESEM images reported in Fig. 1 could explain the higher T_d values registered for the HDPE-Ar974-2 composite. The combustion behavior of nanocomposites filled with various amounts of Aerosil® r974 has been recently investigated also by different techniques, such as cone calorimetry and limiting oxygen index [27].

Tensile mechanical properties

Isothermal creep compliance curves of 2 vol% filled nanocomposites are reported in Fig. 5, while in Table 4 the values of the elastic (D_E) and of the viscoelastic (D_{VE}) compliance at 3600 s are compared. It is immediately evident that the incorporation of fumed silica leads to a decrease in the total

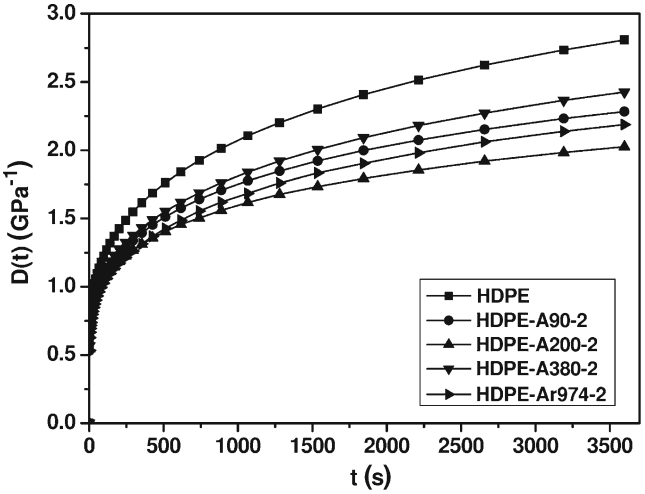

Fig. 5 Creep compliance curves of neat HDPE and nanocomposites with 2 vol% filler content

creep compliance, without any clear dependency from the nanofiller surface area. Analogous effects on the creep behaviour of polymeric nanocomposites observed earlier [28] were attributed to a restriction of the chain mobility due to the dispersion of the nanofiller at the nanoscale. Both the elastic and viscoelastic components of the creep compliance of organosilane treated fumed silica nanocomposite are very similar to those obtained by using untreated nanoparticles at similar surface area. As previously observed in other works in which the tensile creep behaviour of polyolefin nanocomposites filled with functionalized nanoparticles was analyzed, this result could be explained by the assumption of a somewhat higher compliance of the filler–HDPE interphase when surface-treated silica nanoparticle are utilized [1, 2, 29]. In other words, the positive contribution on the nanofiller dispersion induced by the surface functionalization could be partially nullified by the presence of a more compliant filler–matrix interphase.

Figure 6a shows representative stress–strain curves of 2 vol% filled nanocomposites from quasi-static tensile tests at break, while in Table 5 the elastic modulus and the tensile properties at yield (σ_y) and at break (σ_b, ε_b) are collected. All the samples exhibit the typical cold-drawing before the final break of the specimen. During this phenomenon tensile

Table 4 Elastic (D_E), viscoelastic (D_{VE}) and total (D_{TOT}) creep compliance values at 3600 s of polyethylene-fumed silica nanocomposites form isothermal creep tests on 2 vol% samples (T=30 °C, σ_0=10 % σ_y PE)

Sample	D_E (GPa^{-1})	$D_{VE\text{-}3600}$ (GPa^{-1})	$D_{TOT\text{-}3600}$ (GPa^{-1})
HDPE	0.588	2.220	2.808
HDPE-A90-2	0.530	1.753	2.283
HDPE-A200-2	0.546	1.479	2.025
HDPE-A380-2	0.566	1.859	2.425
HDPE-Ar974-2	0.533	1.654	2.187

strength further increases and the stress whitening, due to the crystallization of aligned macromolecules, takes place. As it commonly happens in polyolefin based nanocomposites [23, 30], the introduction of untreated fumed silica in these systems leads to an enhancement of the elastic modulus (+14 % with respect to the neat PE for PE-A380-2 sample). In order to explain the elastic modulus enhancement observed in nanofilled samples, many authors in literature hypothesized the presence of an interphase layer around the nanoparticles, promoting the stress transfer at the interface. It is often reported that the particles can restrict the mobility and deformation of the matrix by introducing a mechanical restraint, caused by an effective attraction potential between segments of the chain and the repulsive potential that the polymer is subjected to when it is close to solid particles. The extent of the particle restriction is a function of the properties of the filler and the matrix [31, 32]. In the present work, DSC tests were performed on nanofilled samples in order to detect the presence of an interphase layer around the particles, but crystallization temperature and crystallinity degree seem to be only slightly affected by the presence of the fillers. Therefore, it can be concluded that the stiffening effect induced by fumed silica nanoparticles could be hardly attributed to the presence of an interphase around the nanoparticles. Alternatively, it is possible to consider the aggregation of the nanoparticles as the mechanism responsible of the observed increase of elastic modulus in nanofilled samples. In other words it can hypothesized that the stiffening effect provided by fumed silica nanoparticles is due to the physical constrain of a certain portion of matrix due to the aggregation of fumed silica nanoparticles. During the production process, primary fumed silica nanobeads, having a mean diameter of about 10–20 nm, tend to physically fuse together to form aggregates during the flame process. These aggregates can form physical agglomerates that can be partially destroyed during the melt compounding process (see Figs. 1 and 2). In any case, the shear forces applied during the melt compounding are not sufficient to disrupt the physical integrity of the aggregates, and the noticeable enhancement of the elastic properties detected for nanofilled samples can be thus attributed to primary aggregation phenomena. In a recent work of our group, a new model, taking into account primary aggregation as the mechanism responsible of the stiffening effect induced by the nanoparticles, was developed to model elastic modulus data of nanofilled samples. A good agreement between theoretical prediction and experimental data was highlighted both for the microcomposites and for the nanofilled samples, and a strong correlation between the filler surface area and the immobilized matrix fraction was detected [33].

Also the tensile stress at yield (σ_y) is positively affected by nanofiller addition. Similar effects were already reported by our group for this HDPE matrix filled with 2 wt% of organoclay [7]. From a general point of view, an enhancement of the yield strength, even if small, is generally considered as an indication of a relatively strong filler-matrix interaction [7, 30], otherwise σ_y would decrease with the introduction of the filler [34, 35]. In fact, as suggested by Galeski et al. [36], in polyolefins filled with traditional microfiller (chalk, calcium carbonate) the increase in the elastic modulus of the material is generally

Table 5 Quasi-static tensile properties of polyethylene-fumed silica nanocomposites (filler content =2 vol%)

Sample	E (GPa)	σ_y (MPa)	σ_b (MPa)	ε_b (%)
HDPE	1.19±0.02	29.6±0.5	24.3±1.4	1381±231
HDPE-A90-2	1.24±0.04	28.8±0.3	29.2±2.6	1528±207
HDPE-A200-2	1.25±0.02	30.4±0.5	30.2±3.6	1580±267
HDPE-A380-2	1.36±0.02	30.2±0.3	28.7±0.8	1528±51
HDPE-Ar974-2	1.24±0.01	31.0±0.6	34.4±0.5	2035±172

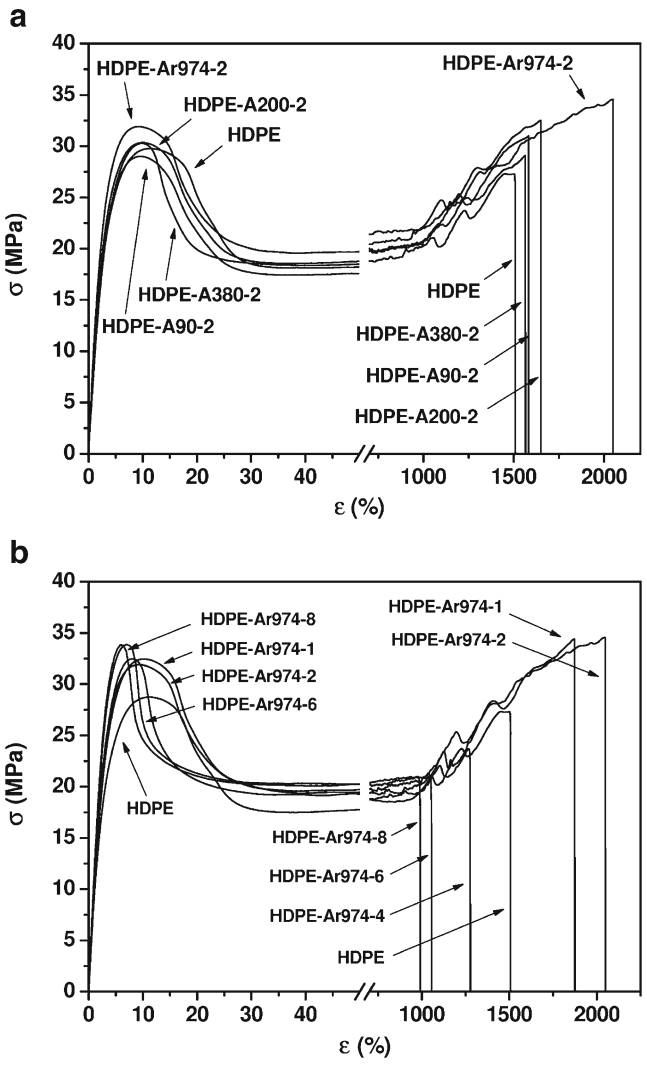

Fig. 6 Representative tensile stress–strain curves of neat HDPE and fumed silica nanocomposites at a cross-head speed of 50 mm·min^{-1}: **a** 2 vol% filled nanocomposites, **b** PE-Ar974-x nanocomposites (x=1–8 vol%)

associated to an heavy decrease of the yield stress, because traditional fillers do not bear the load in the direction of deformation. With regard to the tensile properties at break, it is important to underline that the dispersion of fumed silica nanoparticles at the nanoscale leads to an interesting increase both of σ_b and of the strain at break. In fact, HDPE-Ar974-2 sample shows a σ_b improvement of 10 MPa (i.e. +42 %) compared to neat matrix and a ε_b value higher than 2000 % (i.e. +47 % higher than that of neat HDPE). Considering that in the major part of the works on polyolefin nanocomposites, the stiffening effect due to nanoparticles addition is accompanied by an heavy embrittlement, with a reduction of the tensile properties at break [7], the toughening effect induced by fumed silica nanoparticles can be considered an interesting result confirming the data reported by Kontou and Niaounakis for LLDPE-fumed silica nanocomposite systems [19]. It is likely that the good dispersion of fumed silica aggregates within the matrix may lead to relatively lower stress concentration and cracking nucleation phenomena. Consequently, the smaller dimension of silica aggregates observed for organomodified fumed silica nanoparticles is responsible for a further improvement both of the stress and of the strain at break.

On the basis of the thermo-mechanical characterization performed on 2 vol% nanofilled samples, it emerges that Aerosil® r974 is the more efficient nanofiller in improving both thermo-oxidative resistance and mechanical properties. Therefore, nanocomposites containing various amounts of Aerosil® r974 (from 1 to 8 vol%) were investigated.

Stress–strain curves of neat HDPE and Ar974 filled nanocomposites are reported in Fig. 6b, while in Fig. 7 the trends of the most important mechanical parameters are plotted as a function of silica content. The elastic modulus increases continuously with the filler content. For instance, HDPE-Ar974-8 nanocomposite shows an elastic modulus 46 % higher than that of the neat matrix. The stiffening effect provided by fumed silica nanoparticles can be tentatively modeled by considering the theoretical approaches developed for traditional microcomposites. In particular, the elastic modulus E_c (shear, Young's, or bulk) of a stiff polymer filled with hard, almost spherical particles can be represented by the modified Kerner equation proposed by Lewis and Nielsen [37] in the following form:

$$\frac{E_c}{E_m} = \frac{1 + AB\phi}{1 - \psi B\phi} \tag{1}$$

where :

$$A = \frac{7-5\nu_m}{8-10\nu_m}, \quad B = \frac{\frac{E_p}{E_m}-1}{\frac{E_p}{E_m}+A} \quad \text{and} \quad \psi = 1 + \left(\frac{1-\phi_{max}}{\phi_{max}^2}\right)\phi$$

where Φ is the filler volume fraction, ν_m is the matrix Poisson ratio (0.42 for HDPE [1]), Φ_{max} represents the maximum packing fraction of the filler (0.632 for randomly close packed non-agglomerated spherical particles [35]) while E_p and E_m are the modulus of the particles and of the matrix, respectively. According to this model, the Young's modulus does not explicitly depend on the particle size and particle size distribution. Both these parameters and the effect of surface treatment affect the model previsions only indirectly through the maximum packing fraction (Φ_{max}). The experimental evaluation of the elastic modulus of silica nanoparticles is of considerable difficulty. In literature a value of about 70 GPa is generally reported for amorphous silicon dioxide [38] and therefore we can reasonably adopt it for fumed silica nanoparticles. In Fig. 7a the experimental data are compared with the theoretical previsions according to Lewis-Nielsen model. Generally speaking, it can be observed that the stiffening effect of fumed silica nanoparticles is much higher than that theoretically predicted on the basis of the modified Kerner equation, especially at elevated silica amounts. This result can be explained considering that classical models adopted for microcomposites do not include filler–matrix interactions. On the other hand, these latter phenomena can be important in polymer nanocomposites, in which the interfacial area is much extended. In fact, modification of the filler–matrix interphase region, such as a reduction [39] or an improvement [40] of the polymer chain mobility, was often observed in the case of nanocomposites. As reported in Fig. 7b, also the tensile stress at yield (σ_y) is progressively improved by nanofiller addition, with an enhancement of the 14 % for a silica loading of 8 vol%. In order to investigate the role of the surface functionalization on the yield properties of the investigated composites, it can be interesting to model stress at yield data with the equations commonly utilized in literature to predict the yield strength of particulate filled polymers. The Nicolais-Narkis equation is a two-third power law function with K as a parameter for filler-matrix adhesion [41]:

$$\frac{\sigma_{yc}}{\sigma_{ym}} = 1 - K(\phi)^{2/3} \tag{2}$$

where σ_{yc} and σ_{ym} represent respectively the stress at yield of the composite and of the matrix. This model predicts a decrease of the yield strength of the composite with respect of the pure matrix as the filler amount increases. According to this model, traditionally adopted for particulate filled microcomposites, the stress at yield would gradually decrease with the filler content. As an example, in the case of poor filler-matrix adhesion, 2 vol% filled nanocomposites would have a relative σ_y of 0.91. More recently, the following equation was proposed by Pukanszky et al. [42] :

$$\frac{\sigma_{yc}}{\sigma_{ym}} = \left(\frac{1-\phi}{1+2.5\phi}\right) \cdot \exp(B\phi) \tag{3}$$

where B is an empirical parameter characterizing the degree of filler-matrix interaction. The value of parameter B depends on all factors influencing the load-bearing capacity, i.e. strength and size of the interface. In Fig. 7b the relative tensile stress at

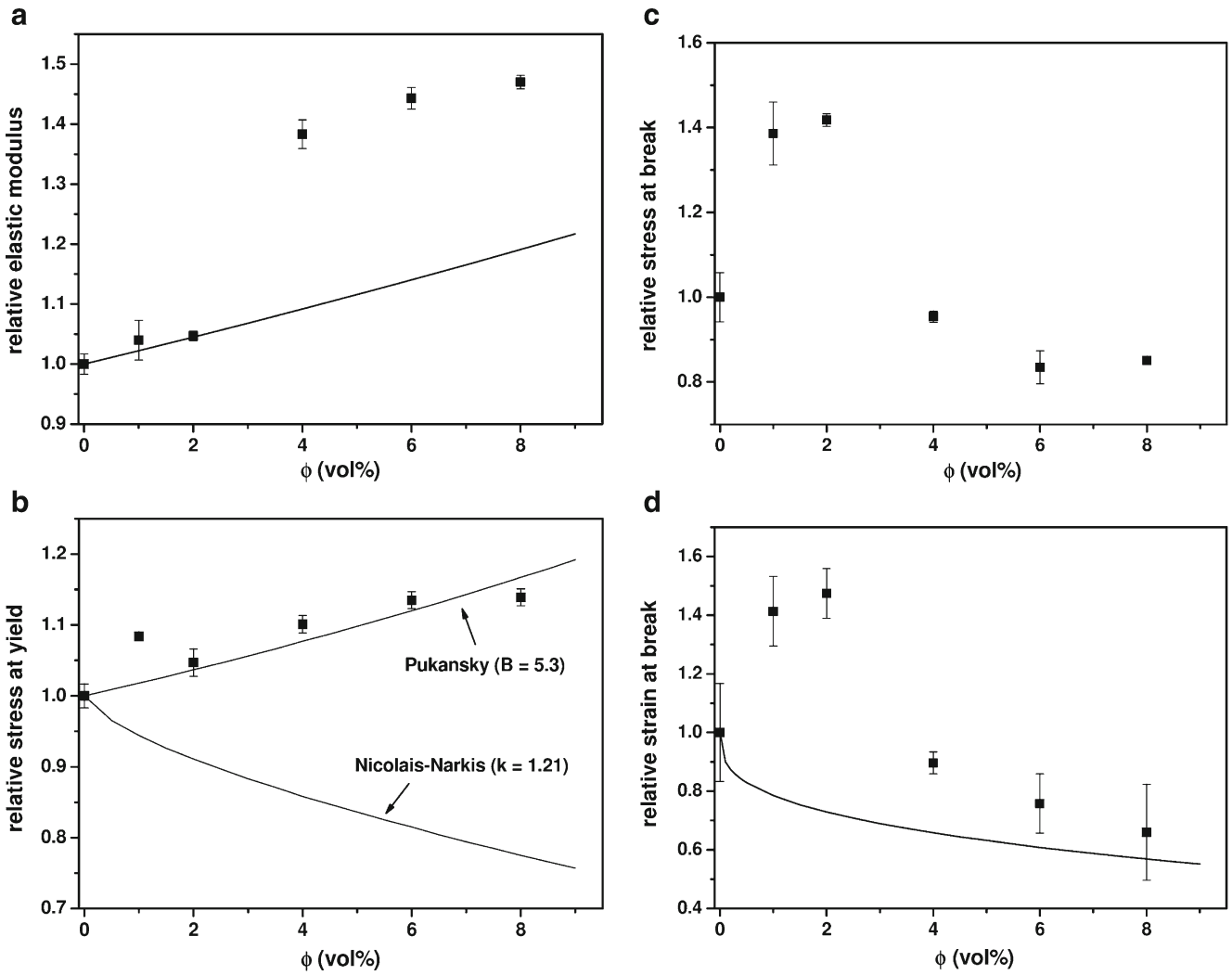

Fig. 7 Quasi-static tensile properties of PE-Ar974-x nanocomposites (x=1–8 vol%) normalized on the neat matrix values. **a** elastic modulus with theoretical prediction according to Lewis Nielsen model (Eq. 1), **b** stress at yield with theoretical prediction according to Nicolais-Narkis (Eq. 2) and Pukansky (Eq. 3) models, **c** stress at break, **d** strain at break with theoretical prediction according to Nielsen model (Eq. 4)

yield data of HDPE and relative composites with the fitting lines according to Pukanszky and Nicolais-Narkis equations are reported. B values of the Pukanszky model were chosen by minimizing chi-square values during the fitting procedure, while for Nicolais-Narkis equation a theoretical K value of 1.21, commonly used in the case of poor filler-matrix adhesion, was utilized. It is evident that Nicolais-Narkis equation is completely unsuitable to describe the yield behaviour of the prepared samples, because negative K values would be necessary to fit yield strength data. The inappreciable significance of the parameters based on these models is attributed to the fact that dynamics of polymer-filler interaction are fundamentally different from the same as in the case of nanocomposites, where the presence of a wide interface alters the physical significance of polymer-filler interaction at the molecular level since structural organization of the matrix at the interface is largerly different from that in the bulk. If a B value of 5.3 is considered, Pukanszky model seems to satisfactorily fit yield stress data. The value found for B parameter is reasonable, considering that generally B parameter for different nanocomposites remains between 2 and 15 [42]. This evidence confirms that the filler-matrix interaction, mainly related to nanofiller dimensions and surface functionalization, plays a key role in these systems. From Fig. 7c–d it can be noticed that both the stress and the strain at break increase up to a silica content of 2 vol%, and then decrease, probably because of the formation of larger aggregates (see FESEM micrographs in Fig. 2c–d). The good dispersion of fumed silica aggregates at the nanoscale level leads to relatively lower stress concentration and cracking nucleation phenomena at the interface up to a filler loading of 2 vol%. The presence of organomodified silica aggregates having a mean size larger than about 100 nm seems to produce a slight embrittlement of the samples. However, the drop experienced in this work is not dramatic, and the properties at break are

lower than that of the neat matrix only at filler loadings higher than 4 vol%. In order to investigate the role of the filler aggregation on the tensile properties at break of the prepared composites, the prediction of Nielsen model [43], originally proposed to model the strain at break of spherical microparticles filled composites with good adhesion between filler, was utilized :

$$\varepsilon_{bc} = \varepsilon_{bm} \cdot \left(1 - \phi^{1/3}\right) \quad (4)$$

where ε_{bc} and ε_{bm} are respectively the strain at break of the composite and of the pure matrix. As reported in Fig. 7d, at filler contents lower than 2 vol% the good dispersion of the nanofiller leads to an interesting enhancement of the strain at break. For higher silica concentrations particles agglomeration produces a ε_b drop up to values near to those theoretically described by Nielsen model, originally developed for microfilled composites.

As recently reported in an extended work on the fracture behaviour of LLDPE/fumed silica nanocomposites [44], a strong orientation of silica aggregates along the elongation direction was observed for strain levels higher than the strain at yield (ε_y) of the polymer matrix. Therefore, it can be hypothesized that the nanoparticles were segregated in the amorphous regions in an aggregated form and separated by crystalline domains. This hypothesis is also supported by the work of Jeol et al. [45] on the deformational behaviour of poly(ethyleneterephtalate)-silica nanocomposites, in which it was concluded that the nanoparticles were rejected from the highly oriented crystalline domains during the strain hardening. In the present case it is therefore probable that the very little width of aligned silica aggregates at elevated deformations is well below the critical defect size for crack nucleation of HDPE, and that the long streams of aggregates along the stress direction may favour load transfer mechanism at the interphase and supplementary energy consumption for their alignment along the strain direction. Another hypothesis is that silica aggregates could play the role of a solid state lubricant. Under these conditions the load sustained by the polymeric phase is reduced and polyethylene macromolecules can deform at an higher extent before breaking.

Conclusions

Various kinds of fumed silica nanoparticles, having different size and surface properties, were added to a high density polyethylene matrix through a melt compounding process, in order to investigate their influence on the thermal degradation resistance and mechanical stability of the resulting materials. Microstructural characterization evidenced that nanoparticles aggregation within the polymer matrix is more pronounced as the nanofiller surface area increases, while nanosilica dispersion was favoured by the presence of an organosilane on the surface of the nanoparticles. Consequently, nanocomposites filled with more hydrophobic fumed silica showed interesting enhancements both of the thermal degradation resistance and of the dimensional stability. A remarkable increment of the stress and strain at break of neat HDPE was also obtained by the addition of 2 vol% silica nanoparticles, especially when surface treated silica was used. The good polymer-filler interfacial interaction obtained by using organomodified nanoparticles led to a progressive enhancement of both elastic modulus and tensile stress at yield with the silica amount, without heavily affecting the original fracture toughness at elevated filler contents.

References

1. Bondioli F, Dorigato A, Fabbri P, Messori M, Pegoretti A (2008) High-density polyethylene reinforced with submicron titania particles. Polym Eng Sci 48:448–457
2. Bondioli F, Dorigato A, Fabbri P, Messori M, Pegoretti A (2009) Improving the creep stability of high-density polyethylene with acicular titania nanoparticles. J Appl Polym Sci 112:1045–1055
3. Cai LF, Lin ZY, Qian H (2010) Dispersion of nano-silica in monomer casting nylon and its effect on the structure and properties of composites. Expr Pol Lett 4(7):397–403
4. Mandalia T, Bargaya F (2005) Organo-clay mineral-melted polyolefin nanocomposites. Effect of surfactant/cec ratio. J Phys Chem Solids 67:836–845
5. Zhang MQ, Rong MZ, Zhang HB, Friedrich K (2003) Mechanical properties of low nano-silica filled high density polyethylene composites. Polym Eng Sci 43(2):490–500
6. Zheng X, Wu D, Meng Q, Wang K, Liu Y, Wan L, Ren D (2007) Mechanical properties of low-density polyethylene/nano-magnesium hydroxide composites prepared by an in situ bubble stretching method. J Polym Res 15(1):59–65
7. Pegoretti A, Dorigato A, Penati A (2007) Tensile mechanical response of polyethylene – clay nanocomposites. Expr Pol Lett 1 (3):123–131
8. Starkova O, Yang JL, Zhang Z (2007) Application of time-stress superposition to nonlinear creep of polyamide 66 filled with nanoparticles of various sizes. Compos Sci Technol 67:2691–2698
9. Tortora M, Gorrasi M, Vittoria G, Galli V, Ritrovati S, Chiellini E (2002) Structural characterization and transport properties of organically modified montmorillonite/polyurethane nanocomposites. Polymer 43(23):6147–6157
10. Zhao C, Qin H, Gong F, Feng M, Zhang S, Yang M (2005) Mechanical, thermal and flammability properties of polyethylen/clay nanocomposites. Polym Degrad Stab 87:183–189
11. Pavlidou S, Papaspyrides CD (2008) A review on polymer-layered silicate nanocomposites. Prog Polym Sci 33(12):1119–1198
12. Peacock AJ (2000) Handbook of polyethylene. Structure, properties and applications. Marcel Dekker, Inc, New York
13. Pegoretti A (2009) Creep and fatigue behaviour of polymer nanocomposites. In: Karger-Kocsis J, Fakirov S (eds) Nano- and micromechanics of polymer blends and composites. Carl Hanser Verlag GmbH & Co. KG, Munich, pp 301–339
14. Sudar A, Moczo J, Voros G, Pukanszky B (2007) The mechanism and kinetics of void formation and growth in particulate filled pe composites. Expr Pol Lett 1(11):763–772

15. Dorigato A, Pegoretti A, Penati A (2010) Linear low-density polyethylene/silica micro- and nanocomposites: dynamic rheological measurements and modelling. Expr Pol Lett 4(2):115–129
16. Dorigato A, Pegoretti A, Kolarik J (2010) Nonlinear tensile creep of linear low density polyethylene/fumed silica nanocomposites: time-strain superposition and creep prediction. Polym Compos 31 (11):1947–1955
17. Dorigato A, Pegoretti A (2010) Tensile creep behaviour of polymethylpentene/silica nanocomposites. Polym Int 59:719–724
18. Dorigato A, Pegoretti A, Fambri L, Slouf M, Kolarik J (2011) Cycloolefin copolymer/fumed silica nanocomposites. J Appl Polym Sci 119(6):3393–3402
19. Kontou E, Niaounakis M (2006) Thermo-mechanical properties of LLDPE/SiO_2 nanocomposites. Polymer 47:1267–1280
20. Mark HF (2004) Encyclopedia of polymer science and technology, 3rd edn. Wiley, New York
21. Chrissafis K, Paraskevopoulos KM, Tsiaoussis I, Bikiaris D (2009) Comparative study of the effect of different nanoparticles on the mechanical properties, permeability, and thermal degradation mechanism of hdpe. J Appl Polym Sci 114:1606–1618
22. Sinha Ray S, Okamoto M (2003) Polymer/layered silicate nanocomposites: a review from preparation to processing. Prog Polym Sci 28:1539–1641
23. Barus S, Zanetti M, Lazzari M, Costa L (2009) Preparation of polymeric hybrid nanocomposites based on pe and nanosilica. Polymer 50:2595–2600
24. Alexandre M, Dubois P (2000) Polymer-layered silicate nanocomposites: preparation, properties and uses of a new class of materials Mater Sci Eng. R 28:1–63
25. Morgan AB (2006) Flame retarded polymer layered silicate nanocomposites: a review of commercial and open literature systems. Polym Adv Technol 17:206–217
26. Garcia N, Hoyos M, Guzman J, Tiemblo P (2009) Comparing the effect of nanofillers as thermal stabilizers in low density polyethylene. Polym Degrad Stab 94:39–48
27. Dorigato A, Pegoretti A, Frache A (2012) Thermal stability of high density polyethylene-fumed silica nanocomposites. J Therm Anal Calorim. doi:10.1007/s10973-012-2421-4
28. Zhang Z, Yang JL, Friedrich K (2004) Creep resistant polymeric nanocomposites. Polymer 45:3481–3485
29. Dorigato A, Pegoretti A, Migliaresi C (2009) Physical properties of polyhedral oligomeric silsesquioxanes–cycloolefin copolymer nanocomposites. J Appl Polym Sci 114:2270–2279
30. Ranade A, Nayak K, Fairbrother D, D'Souza NA (2005) Maleated and non maleated polyethylene-montmorillonite layered silicate blown films: Creep, dispersion and cristallinity. Polymer 46:7323–7333
31. Fu SY, Xu G, Mai YW (2002) On the elastic modulus of hybrid. Particle/short fiber/polymer composites. Compos B 33:291–299
32. Drozdov AD, Dorfmann A (2001) The stress–strain response and ultimate strength of filled elastomers. Comput Mater Sci 21:395–417
33. Dorigato A, Dzenis Y, Pegoretti A (2011) Nanofiller aggregation as reinforcing mechanism in nanocomposites. Procedia Engineering 10:894–899
34. Ahmed S, Jones FR (1990) A review of particluate reinforcement theories for polymer composites. J Mater Sci 25(12):4933–4942
35. Nielsen LE, Landel RF (1994) Mechanical properties of polymers and composites. Dekker, New York
36. Galeski A (2003) Strength and toughness of crystalline polymer systems. Prog Polym Sci 28:1643–1699
37. Lewis TB, Nielsen LE (1970) Dynamic mechanical properties of particulate-filled composites. J Appl Polym Sci 14:1449–1471
38. Klocek P (1991) Handbook of infrared optical materials. Dekker, New York
39. Ciprari D, Jacob K, Tannenbaum R (2006) Characterization of polymer nanocomposite interphase and its impact on mechanical properties. Macromolecules 39:6565–6573
40. Miltner HE, Rahier H, Pozsgay A, Pukanszky B, Van Mele B (2005) Experimental evidence for reduced chain segment mobility in poly(amide)-6/clay nanocomposites. Compos Interfaces 12:787–803
41. Nicolais L, Nicodemo L (1973) Polym Eng Sci. Strength of particulate composite 13:469–477
42. Szazdi L, Pukanszky BJ, Vancso GJ, Pukanszky B (2006) Quantitative estimation of the reinforcing effect of layered silicates in pp nanocomposites. Polymer 47:4638–4648
43. Nielsen LE (1966) Simple theory of the stress–strain properties of filled polymers. J Appl Polym Sci 10:97–103
44. Dorigato A (2009) Viscoelastic and fracture behaviour of polyolefin based nanocomposites. PhD Disssertation, University of Trento
45. Jeol S, Fenouillot F, Rousseau A, Masenelli-Varlot K, Gauthier C, Briois J (2007) Drastic modification of the dispersion state of submicron silica during biaxial deformation of poly(ethyleneterephthalate). Macromolecules 40:3229